TECHNISCHE MECHANIK, Band 19, Heft 2, (1999), 115-126
Manuskripteingang: 30. Juli 1998

Adaptive Local-Global Analysis by pNh Transition Elements

U. Gabbert, K. Graeff-Weinberg

The paper presents a new family of finite transition elements, which we named pNh-elements. The pNh-elements are especially designed for a compatible transition from a h-refined to a p-refined mesh region. At one or more sides of a pNh-element a h-discretization with N piecewise defined shape functions are combined with a p-extension at the remaining parts of the element. The elements pass the patch test and can be used in an adaptive finite element scheme, where an extended Babuška error indicator has proved to be reliable. The proposed pNh-elements have been tested within a special finite element code as well as a commercial code. A number of numerical tests and real engineering examples demonstrate the suitability, especially if local mesh refinements are required (e.g. multiscale problems, contact problems).

1 Introduction

A finite element software is expected to solve a given engineering problem as accurately as necessary at reasonable cost. In addition the creation of a good mechanical model should be automatically supported by the software. We believe that software products based on intelligent finite element techniques will dominate the future software market. Due to the extensive research and development activities in the recent decade carried out by engineers and mathematicians a good theoretical basis exists for future developments in the direction of more intelligent finite element technologies. Very important milestones are the developments in the field of error estimation by Babuška and Rheinbold (1978), Zienkiewicz and Zhu (1987, 1992) and the work in the field of h-, p-, hp-, r- and s-adaptivity resulting in series of important papers (see e.g. Babuška, 1988; Oden et al., 1989; Szabo and Babuška, 1991; Fish, 1992; Wiberg, 1994). The discretization error of a given finite element model can be accurately calculated by a posteriori error estimation techniques, which are the basis for an adaptive h- and/or p-extension. With respect to large engineering problems it is nearly impossible to carry out several analysis steps before achieving a certain accuracy. Based on a priori knowledge about the behaviour of the solution an optimal locally refined initial mesh can be created automatically, which leads to a considerable reduction of further adaptation steps (see Gabbert and Zehn, 1995). The accuracy of finite element results depends not only on the discretization error, but is significantly affected by the created mathematical model, i.e. the dimension of the model (e.g. 1D, 2D, 2 ½D, 3D) and the quality of the model (e.g. Bernoulli or Thimoshenko beam theory, Kirchhoff or Mindlin plate theory etc.). The important contribution of Stein (see e.g. Stein et al., 1993, 1995, Jensen, 1990) has opened the door to a practical application of a mathematically well founded dimensional and model adaptivity which is one of the major steps on the way to intelligent finite element technologies. Finally, except of the mathematical projection error the quality of the numerical simulation of real engineering problems depends on the physical projection error, which has to be assessed by measured data. Consequently, a combination of updating the mathematical as well as the physical model (see e.g. the survey given by Mottershead and Friswell, 1993; Gabbert et al., 1995) seems to be the best way leading to reliable simulation results. Unfortunately, only few of the actual research results are incorporated into commercial finite element codes. Among other things, this is caused by a number of specific problems in practical applications, which are yet unsolved. In linear elasticity – the most used model in solid mechanics applications – a combination of the h- and the p-adaptive version has proved to be the best finite element strategy with respect to the discretization error and the convergency rate (see e.g. Oden et al., 1989; Szabo and Babuška, 1991). Oden et al. (1989) developed a strategy for choosing local mesh size and polynomial degrees to reduce elementwise errors below a given tolerance. By means of hierarchical shape functions and mesh refinements from one to two elements with constraint conditions for the hanging nodes convincing results have been presented for simply shaped geometries. In real engineering problems the behaviour of the solution is often characterised by smooth functions of the field variables (e.g. stresses, displacements, temperatures etc.) in most parts of the solution region and singular or nearly singular behaviour in other parts (e.g. due to material inclusions, cracks, contact etc.). Often a very dense h-discretization is required in these local regions to achieve a prescribed accuracy. An application of an optimal combined h- and p-adaptive finite element technique requires a very flexible interface for the coupling of h- and p-refined mesh regions. The usual mesh refinement techniques (see Figure 1) are not very flexible in grading the mesh (especially in 3D applications). They lead to artificial mesh distortions and are difficult to apply in the p-version. Alternatively, an incompatible mesh refinement technique can be used, where the penalty method or Lagrangian multipliers are used to fulfil the constraint conditions. The main disadvantage of this technique is the loss of accuracy in the local region caused by the constraints.

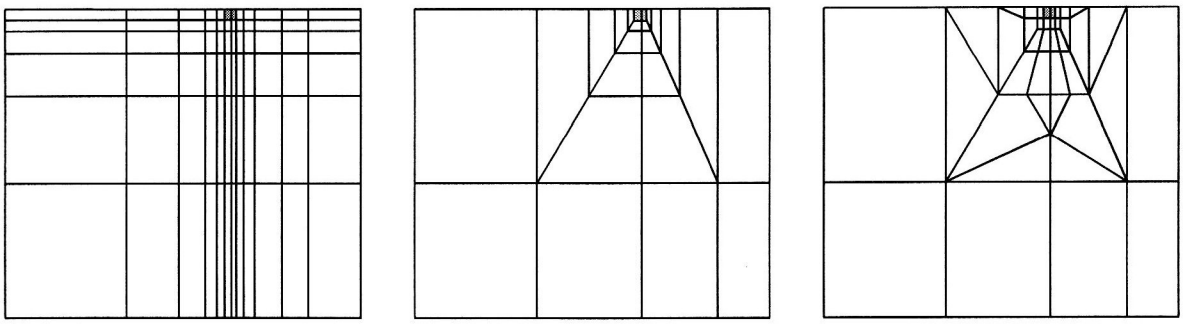

Figure 1. Usual Mesh Refinement Techniques in 2D Problems

To overcome the problems in coupling h- and p-refined regions we created a new transition element concept, which allows a flexible connection of any p-type element with any number of usual h-elements and consequently, the desirable local mesh refinement of Figure 1 can be obtained in a manner shown in Figure 2.

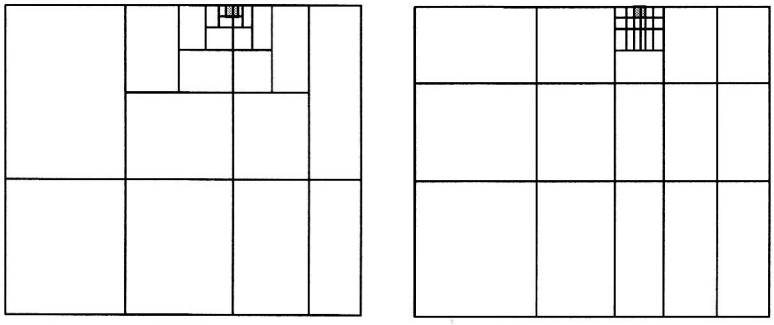

Figure 2. Mesh Refinement by Special Transition Elements

The transition elements are special p-version elements with the usual hierarchical polynomial shape functions, which are able to generate any number N of piecewise defined h-discretizations at one or more sides or faces of the element. Therefore the name *pNh-transition element* is self-explanatory. In Figure 3 the very flexible coupling of a h-refined mesh domain with a p-type mesh domain is demonstrated. It is not necessary to divide the h-refined side of the pNh-element into sections of equal length and the polynomial degree can also be different at every h-part.

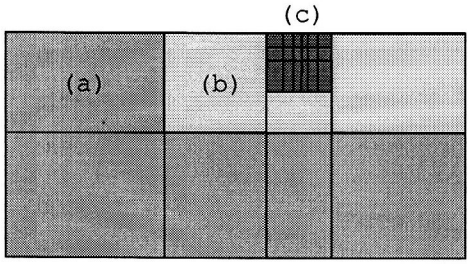

Figure 3. Domain Decomposition in (a) p-Type, (b) pNh-Type and (c) h-Type Elements

2 Theoretical Basis of the pNh-Elements

As we mentioned above the pNh-elements can be considered as special p-type finite elements. The usual p-elements extend the linear finite element function space by additional shape functions of higher polynomial degree. It has been proved (see Szabo, et al. 1991) that hierarchical functions as additional shape functions have a beneficial influence on the numerical properties of the problem (e.g. condition number of the stiffness matrix). Consequently, we use the Legendre polynomials

$$P_n(x) = \frac{1}{2^n n!}\frac{d^n}{dx^n}\left(x^2-1\right)^n \tag{1}$$

to construct the p-type additional shape functions by the normalised integrals of $P_n(x)$:

$$\phi_n(\xi) = \sqrt{\frac{(2n-1)}{2}} \int_{x=-1}^{\xi} P_{n-1}(x)dx \qquad n \geq 2 \tag{2}$$

which result in $\phi_2 = \frac{1}{4}\sqrt{6}\left(\xi^2-1\right)$, $\phi_3 = \frac{1}{4}\sqrt{10}\left(\xi^3-\xi\right)$, $\phi_4 = \frac{1}{16}\sqrt{14}\left(5\xi^4-6\xi^2+1\right)$,

$\phi_5 = \frac{1}{16}\sqrt{18}\left(7\xi^5-10\xi^3+3\xi\right)$, $\phi_6 = \frac{1}{96}\sqrt{22}\left(63\xi^6-105\xi^5+45\xi^2-3\right)$ etc.

From the definition of ϕ_n and the orthogonality properties of the Legendre polynomials we have:

$$\phi_n(-1) = \phi_n(+1) \qquad n = 2,3,... \tag{3}$$

and

$$\int_{-1}^{1} \frac{\partial\phi_m}{\partial\xi}\frac{\partial\phi_n}{\partial\xi}d\xi = \begin{cases} 0 & \text{for } m \neq n \\ 1 & \text{for } m = n \end{cases} \tag{4}$$

2.1 Standard p-Element as Basis for the pNh-Elements

Exemplary in the following we give a general description of the displacement approximate functions $\tilde{u}_i(\xi_1,\xi_2,\xi_3)$, $i = 1,2,3$ of a C_0 continuous hexahedron element (see Figure 4) of the polynomial degree p, which consists of corner-modes, edge-modes, face-modes and inner-modes:

$$\underbrace{\tilde{u}_i(\xi) = \sum_{c=1}^{8} G_c(\xi)\cdot\hat{u}_{ic}}_{G(\xi)} + \underbrace{\sum_{e=1}^{12}\sum_{n=2}^{p} A_{en}(\xi)\cdot a_{ien}}_{A(\xi)} + \underbrace{\sum_{f=1}^{6}\sum_{m=2}^{p-2}\sum_{n=2}^{p-m} B_{fmn}(\xi)\cdot b_{ifmn}}_{B(\xi)} + \underbrace{\sum_{l=2}^{p-4}\sum_{m=2}^{p-1}\sum_{n=2}^{p-1-m} C_{lmn}(\xi)\cdot c_{ilmn}}_{C(\xi)} \tag{5}$$

linear corner-modes p-edge-modes p-face-modes p-inner-modes

The $\hat{u}_{ic}, a_{ien}, b_{ifmn}, c_{ilmn}$, $i = 1, 2, 3$ are the unknown parameters of the approximate function, where only the $\hat{u}_{ic}$ have a real physical meaning namely the eight displacements at the corners $(\xi_i = \pm 1)$ and the $G_c, A_{en}, B_{fmn}, C_{lmn}$ are the shape functions of the corner modes, edge modes, face modes and inner modes respectively, which are constructed as follows.

Corner modes
With the linear functions in natural co-ordinates

$$g_c(\xi_i) = \frac{1}{2}(1+\xi_{ic}\xi_i) \tag{6}$$

where ξ_{ic} are the local co-ordinates at the eight corners (c = 1,2, ..., 8) we get the eight standard shape functions of a eight node hexahedron

$$G_c(\xi_1,\xi_2,\xi_3) = g_c(\xi_1)\cdot g_c(\xi_2)\cdot g_c(\xi_3) \tag{7}$$

Edge modes
At every edge of the hexahedron functions of higher order $(p \geq 2)$are defined, which are multiplied by linear functions in the remaining directions resulting in a sum of $12\,(p-1)$shape functions for the twelve edges. For the edge $e = 1$ (see Figure 4) the shape functions are

$$A_{1n}(\xi_1,\xi_2,\xi_3) = \phi_n(\xi_1)\cdot g_1(\xi_2)\cdot g_1(\xi_3) \tag{8}$$

Face modes

At every face of a hexahedron the product of one dimensional functions of higher order degree $(p \geq 4)$in the local face co-ordinate system are multiplied by a linear function in the remaining direction resulting in a sum of $6\frac{1}{2}(p-2)(p-3)$shape functions for the six faces. For the face $f=1$(see Figure 4) the shape functions are

$$B_{1mn}(\xi_1,\xi_2,\xi_3) = \phi_m(\xi_1) \cdot \phi_n(\xi_2) \cdot g_1(\xi_3) \tag{9}$$

Inner modes

In all three local co-ordinate directions the product of one dimensional functions of higher order degree $(p \geq 6)$results in $\frac{1}{6}(p-3)(p-4)(p-5)$shape functions of the type

$$C_{lmn}(\xi_1,\xi_2,\xi_3) = \phi_l(\xi_1) \cdot \phi_m(\xi_2) \cdot \phi_n(\xi_3) \tag{10}$$

The above defined shape functions are continuous and differentiable over the total element region and due to equation (3) every individual function vanishes at those corners, edges and faces respectively where they are not related to. The construction of the shape functions of the quadrilateral element follows from equation (5) neglecting the ξ_3 co-ordinate. Other element types (triangular, tetrahedron, pentahedron etc.) can be constructed in a similar way.

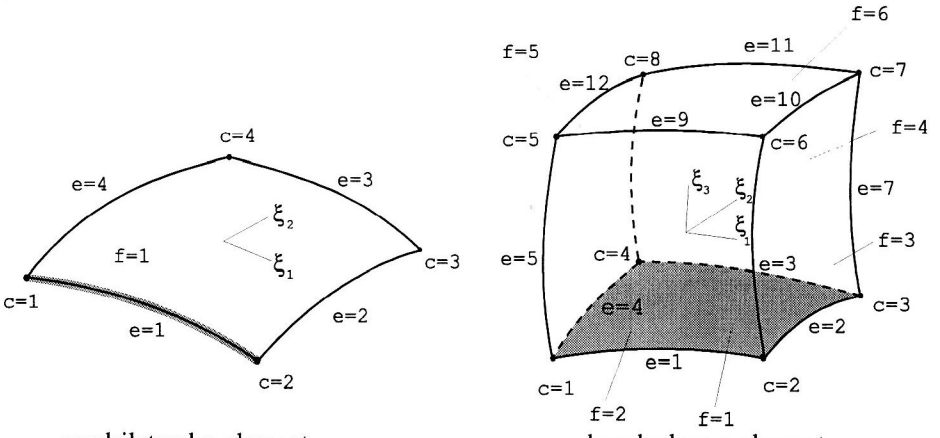

quadrilateral p-element hexahedron p-element

Figure 4. Standard Quadrilateral and Hexahedron p-Type Elements (c – corner, e – edge, f – face)

2.2 Shape Functions of the pNh-Elements

The pNh-elements differ from the standard p-elements by an alternative piecewise formulation of the shape functions at one or more edges or faces. At these so called Nh-edges or Nh-faces nodes are introduced, which span the piecewise functions in a manner that they are compatible with lower order elements. Consequently, a compatible coupling of one p-elements with any elements of normally lower order shape functions is possible (see Figure 3). Of course this concept is not restricted to p-type elements as basic, which are preferable because of the better numerical properties. Also node based Lagrangian or Serendipity elements can be used as basis for the development of pNh-elements (see Figure 5).

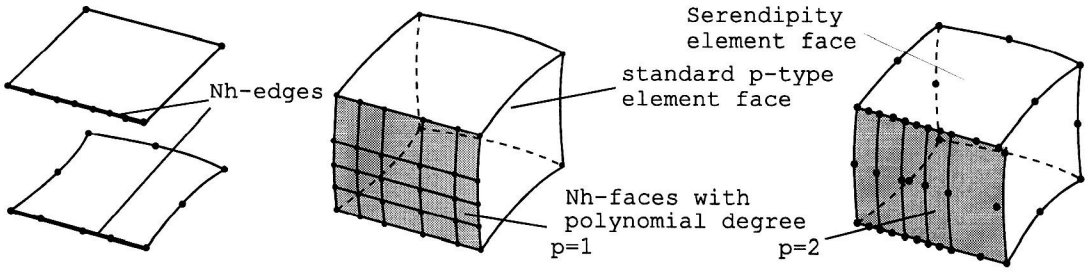

Figure 5. Different Types of pNh-Transition Elements

The construction of the shape functions of the pNh-elements requires only to change those parts of the general approximate function of a p-type element in equation (5), which are related to the Nh-edges or Nh-faces of the element. We assume that the edge $e = 1$ (Figure 4) is a Nh-edge subdivided in n = 1 ,..., N parts with piecewise linear and quadratic shape functions respectively (see Figure 6).

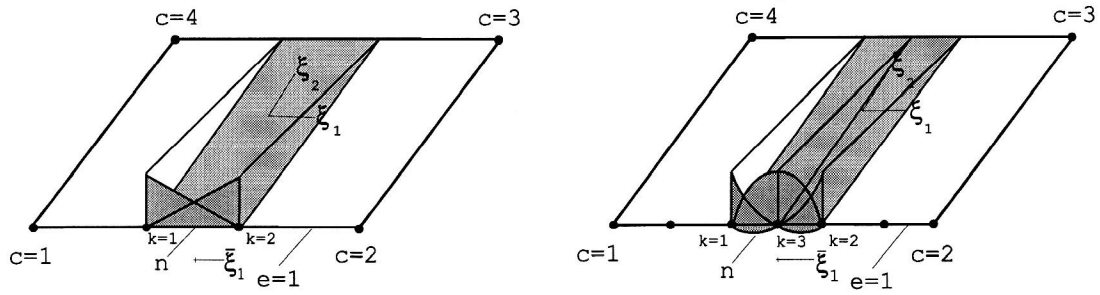

Figure 6. Standard Linear and Quadratic Functions at the n-th Part of a Nh-Edge

At the n-th part, which is bounded by the nodes $\xi_1^{(n)} \in \left[\xi_{11}^{(n)}, \xi_{12}^{(n)}\right]$, we define a local co-ordinate system (see Figure 6)

$$\bar{\xi}_1^{(n)} = \frac{1}{\Delta\xi_1^{(n)}}\left(\xi_{11}^{(n)} + \xi_{12}^{(n)} - 2\xi_1^{(n)}\right) \tag{11}$$

with $\bar{\xi}_1^{(n)} = \in \left[\bar{\xi}_{11}^{(n)}, \bar{\xi}_{12}^{(n)}\right] = \in [-1,+1]$ and $\Delta\xi_1^{(n)} = \xi_{12}^{(n)} - \xi_{11}^{(n)}$. Based on these definitions the standard shape functions of a h-type part of a p-element can be described. For the Nh-modes at edge e = 1 the p-edge-modes $A(\xi)$in equation (5) changes as follows:

$$\underbrace{A(\xi) = \sum_{e=1}^{1}\sum_{n=1}^{N}\left[\sum_{k=1}^{K(n)} G_k^{(n)}\left(\bar{\xi}_1^{(n)}, \xi_2, \xi_3\right)\cdot u_{iek}^{(n)}\right]}_{\text{Nh-edge-modes at } e=1} + \underbrace{\sum_{e=2}^{12}\sum_{n=2}^{p} A_{en}(\xi)\cdot a_{ien}}_{\text{remaining p-edge-modes}} \tag{12}$$

where $K^{(n)}$ is the number of nodes at the n-th part of the Nh-edge (linear case: $K^n = 2$, quadratic case: $K^{(n)} = 3$), $u_{iek}^{(n)}$ are the displacements at the nodes of the n-th part and G_k are the shape functions

$$G_k^{(n)}\left(\bar{\xi}_1^{(n)}, \xi_2, \xi_3\right) = g_1\left(\bar{\xi}_1^{(n)}\right)\cdot g_1(\xi_2)\cdot g_1(\xi_3) \tag{13}$$

In the linear case k = 1, 2 we have

$$g_1 = \frac{1}{2}\left(1 - \bar{\xi}_1^{(n)}\right) \qquad g_2 = \frac{1}{2}\left(1 + \bar{\xi}_1^{(n)}\right) \tag{14}$$

and in the quadratic case $k = 1, 2, 3$ we have

$$g_1 = -\frac{1}{2}\bar{\xi}_1^{(n)}\left(1 - \bar{\xi}_1^{(n)}\right) \qquad g_2 = \frac{1}{2}\bar{\xi}_1^{(n)}\left(1 + \bar{\xi}_1^{(n)}\right) \qquad g_3 = 1 - \left(\bar{\xi}_1^{(n)}\right)^2 \tag{15}$$

Analogous to the edge-modes the Nh-face-modes can be developed. For the face $f = 1$ (see Figure 4) with a local N x M mesh of standard shape functions (e.g. linear or quadratic) we can write $B(\xi)$in equation (5) as follows:

$$B(\xi) = \underbrace{\sum_{f=1}^{1}\sum_{n=1}^{N}\sum_{m=1}^{M}\left[\sum_{k=1}^{K^{(n,m)}} G_k^{(n,m)}\left(\bar{\xi}_1^{(n)}, \bar{\xi}_2^{(m)}, \xi_3\right)\cdot \hat{u}_{i1k}^{(n,m)}\right]}_{(N \text{ x } M) \text{ h-face-modes at } f=1} + \underbrace{\sum_{f=2}^{6}\sum_{m=2}^{p-2}\sum_{n=2}^{p-m} B_{fmn}(\xi)\cdot b_{ifmn}}_{\text{remaining p-face-modes}} \qquad (16)$$

where $G_k^{(n,m)}$ are for instance standard Lagrangian or Serendipity shape functions (see e.g. Zienkiewicz, 1977) of the (n,m)-th part of the face $f = 1$, which are described in local co-ordinates $\bar{\xi}_1^{(n)}, \bar{\xi}_2^{(m)}$ (see Figure 7), $\hat{u}_{ijk}^{(n,m)}$ are the displacements at the $K^{(n)}$ nodes of the (n, m)-th part of the Nh-face (e.g. linear case: $K^{(n,m)} = 2$, quadratic case: $K^{(n)} = 8$ for Serendipity elements).

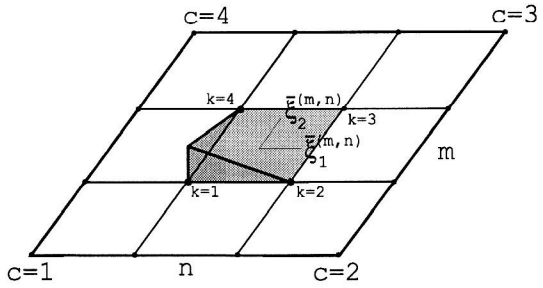

bilinear Nh-function

Figure 7. Bilinear Shape Function at a Nh-Face

It has to be taken into account that the shape functions given above include the linear corner functions at the corners bounding a Nh-edge or a Nh-face and consequently this corners have to be deleted in the function $C(\xi)$ of equation (5). The Figure 6 and 7 demonstrate that the approximate functions at the pN-parts of the element are piecewise defined C_0 continuous functions with uncontinuous first derivatives. The calculation of the element stiffness matrices and load vectors requires a piecewise numerical integration. For the approximation of the geometry the standard concepts, e.g. the iso-, sub- or superparametric mapping techniques (Zienkiewicz, 1977), the blending function method (see Gordon, 1971; Szabo et al, 1991) are suitable. We use the blending function method to describe curved element boundaries of the p-elements and pNh-elements (see Graeff-Weinberg, 1995).

3 Error Estimation and Accuracy of the Elements

The pNh-elements have been designed for applications in a hp-adaptive finite element schema, which requires an reliable error estimation for these elements. According to our experiences in h-adaptive techniques (see Mücke, 1992; Gabbert et al, 1995; Fels, et al. 1992) we use the residual error estimation method originally developed by Babuška and Rheinbold (1978), which has proved to be reliable and accurate. If we use the principal of minimum potential energy

$$\begin{aligned}\pi(\tilde{\mathbf{u}}) &= \frac{1}{2}\int_V \boldsymbol{\varepsilon}^T(\tilde{\mathbf{u}})\cdot\boldsymbol{\sigma}(\tilde{\mathbf{u}})\,dV - \int_V \tilde{\mathbf{u}}^T\cdot\bar{\mathbf{p}}\,dV - \int_{O_q}\tilde{\mathbf{u}}^T\cdot\bar{\mathbf{q}}\,dV \\ &= \frac{1}{2}\int_v (\mathbf{D}\tilde{\mathbf{u}})^T\cdot\mathbf{E}\cdot(\mathbf{D}\tilde{\mathbf{u}})\,dV - \int_V \tilde{\mathbf{u}}^T\cdot\bar{\mathbf{p}}\,dV - \int_V \tilde{\mathbf{u}}^T\cdot\bar{\mathbf{q}}\,dV \\ &= \frac{1}{2}a(\tilde{\mathbf{u}},\tilde{\mathbf{u}}) - b(\tilde{\mathbf{u}})\end{aligned} \qquad (17)$$

where $\boldsymbol{\varepsilon}$ is the strain vector, $\boldsymbol{\sigma}$ is the stress vector, $\bar{\mathbf{p}}$ and $\bar{\mathbf{q}}$ are prescribed body and distributed loads respectively, $\mathbf{D}$ is the strain displacement relation and $\mathbf{E}$ is the Hooke's matrix. If we approximate the displacement field by admissible approximate functions $\tilde{\mathbf{u}}$, which span the finite element space, the minimum of potential energy equation (17)

$$\delta\pi(\tilde{\mathbf{u}}) = 0 \text{ with } \boldsymbol{\sigma} = \mathbf{D}\tilde{\mathbf{u}} \text{ in } V \text{ and } \tilde{\mathbf{u}} = \bar{\mathbf{u}} \text{ at } O_u \qquad (18)$$

gives an error $\mathbf{e} = \mathbf{u} - \tilde{\mathbf{u}}$, which can be measured in the energy norm

$$\|\mathbf{e}\|_E = \sqrt{a(\mathbf{e},\mathbf{e})} \tag{19}$$

The solution $\tilde{\mathbf{u}}$ calculated by minimising the potential energy gives an approximate solution of the static equilibrium equations and the static boundary conditions

$$\mathbf{D}^T\boldsymbol{\sigma}_S + \bar{\mathbf{p}}_S = \mathbf{R}_S \qquad \text{in } \Omega_S \tag{20}$$

$$\mathbf{t}_S^+ + \mathbf{t}_S^- = \mathbf{J}_S \qquad \text{at } \Gamma_S \tag{21}$$

where Ω_S and Γ_S are a subdomain and the boundary of this subdomain respectively (normally identically with a finite element), $\mathbf{R}_S$ is the residuum vector of the equilibrium equation in Ω_S and $\mathbf{J}_S$ is the jump between the traction vectors $\mathbf{t}_S$ of neighbouring regions connected by the same boundary Γ_S (i.e. the lack in the stress continuity condition). Following the standard strategy of Babuška et al. (1978, 1988) the error estimator η_s of every subdomain is

$$\eta_S^2 = C \cdot \left[h_S^2 \int_{\Omega_S} \mathbf{R}_S^T \cdot \mathbf{R}_S d\Omega + c \cdot h_S \int_{\Gamma_S} \mathbf{J}_S^T \cdot \mathbf{J}_S d\Gamma \right] \tag{22}$$

Here h_S is a characteristic length of the subdomain (we use the cube root of Ω_S), the constants C depends on the dimension and the elastic constants and c depends on the type of the boundary (interelement boundary: $c = 1/2$, boundary with prescribed loads: $c = 1$, boundary with prescribed displacements: $c = 0$, see Mücke, 1992). The error indicator describes the relative contribution of the subdomain to the total error. In an adaptive finite elements version an extension of the finite element space is used to correct the total error given by the sum

$$\eta^2 = \sum_{(S)} \eta_S^2 \tag{23}$$

to get an estimation of the error in the energy norm $\|\mathbf{e}\|_E^2$. We use an extrapolation technique (see e.g. Szabo, 1991), which gives an good error estimation also in the pre-asymptotic range. In standard elements the subdomains are the elements itself. The special construction of the shape functions of the pNh-elements results in several element subdomains (see Figure 8) and consequently in all subdomains an error estimator equation (22) has to be calculated and added up to the element error indicator. The specification of the standard residual error estimation technique for pNh-elements has been tested at numerous hp-adaptive finite element analyses and the results have demonstrated the accuracy of the estimation (see Graeff-Weinberg, 1996). In the application of pNh-elements the question of an optimal relation between the polynomial degree and the number of Nh-parts. A general mathematical answer of the question has not been found yet.

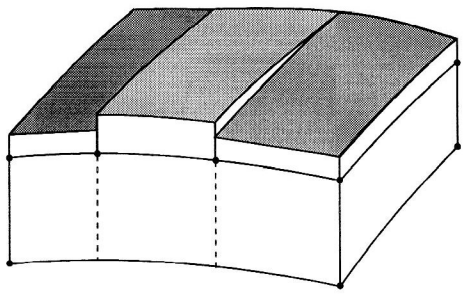

Figure 8. Stress Distribution in the Subdomains of a pNh-Element

Numerical tests have given the expected result, that a one-sided increasing of either the polynomial degree p of the shape functions in the element or the number of Nh-parts (with fixed or lower order polynomial degrees of p=1 or p=2) at the Nh-side result in looking of the accuracy and consequently, a locking of the convergence rate. The optimal relationship between p and N depends on the type of the problem (e.g. the regularity of the solu-

tion). The following example demonstrates the typical behaviour. We investigate the accuracy of the pNh-approximation of a given function

$$u(x_1, x_2) = C \cdot r^{-0.5} = C \cdot \left(x_1^2 + x_2^2\right)^{-0.5} \tag{24}$$

over the quadrilateral region given in Figure 9. The pNh-element has one Nh-edge subdivided in N parts with linear shape functions and complete polynomial functions of degree p at the remaining edges and the element inside. The total number of degrees of freedoms is then

$$NFG = N + \frac{5}{2}p + \frac{1}{2}p^2 \tag{25}$$

Figure 9 demonstrates how the error in the L^2 -Norm

$$\|e\|_{L^2} = \|u - \tilde{u}\|_{L^2} \tag{26}$$

depends on the polynomial degree p and the number linear functions at the Nh-edge. Obviously the error decreases rapidly with p=1 to p=4 and N=2 to N=10, but a further increase of p or N has an insignificant influence on the error reduction. Similar results have been achieved in several numerical investigations in the L^2 -Norm as well as in the energy-norm.

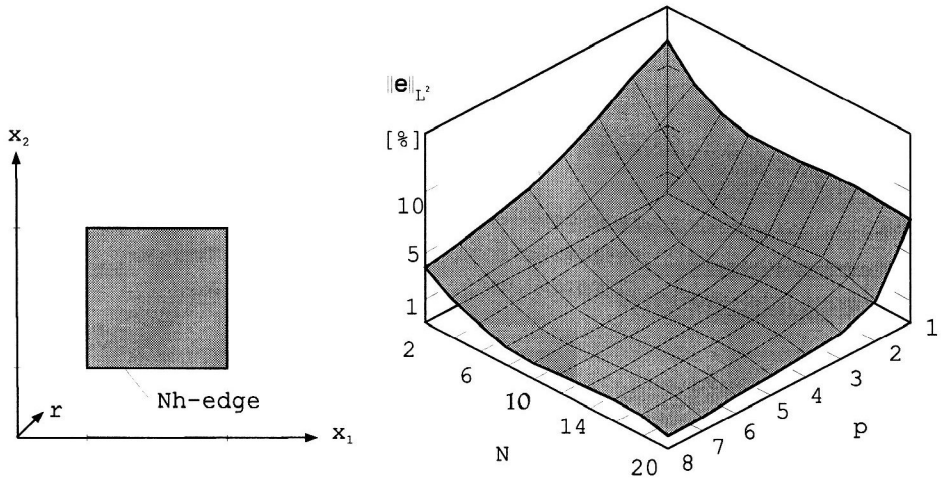

Figure 9. Quality of Approximation of a pNh-Element in Dependence on the Polynomial Degree p and the Number N of Linear Functions

4 Numerical Tests and Engineering Applications

The developed 2D and 3D pNh-transition elements have been implemented in a special purpose p-version code and the general purpose h-version finite element system COSAR. The form of the approximate functions of the pNh-elements given above is suitable to develop general subroutines to build the stiffness, mass and load matrices for 2D and 3D elements, which can be incorporated into standard finite element codes. It has been demonstrated that under appropriate circumstances (e.g. object-oriented data and module structure) the p-version and the pNh-elements can be simply incorporated in a h-version finite element analysis code. But the application of the pNh-elements in real engineering problems also requires its integration into pre-processing (e.g. automatic mesh generation) and the post-processing. In the following we present same examples, which demonstrate the possibilities and advantages of the new element family.

4.1 Plane Strain Problem with a Crack

As a first example a symmetric plane strain crack problem is shown in Figure 10. In Figure 11 we compare the results of a uniform h-extension (linear shape functions) and a uniform *p*-extension starting from a 2 x 2 mesh with locally restricted h-extension. In the latter variant, which is named pNh-refinement in Figure 11, only the elements in the h-mesh region have been quartered from a 2 x 2 to a 7 x 7 subdivision. The p-mesh region remains unchanged (p=2) and consequently pNh-elements have to be used with an increasing number of Nh-parts at the coupling edges. The comparison of the three variants in Figure 11 demonstrate that suitable results can be achieved in embedding a local h-mesh in a p-mesh.

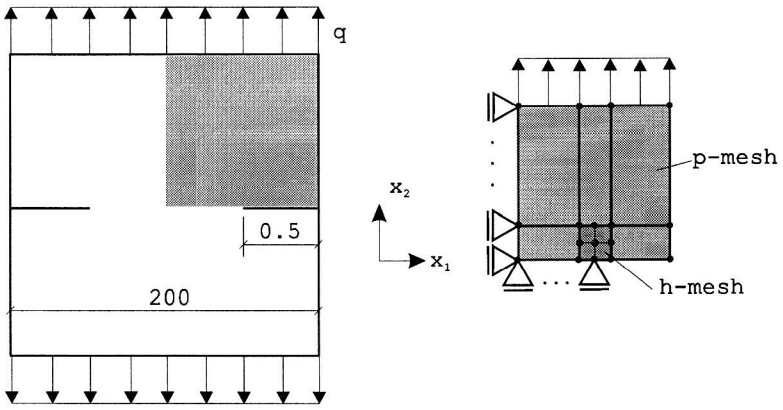

Figure 10. Symmetric Plane Strain Problem with Two Cracks and Initial Mesh, with q=1, E=1, μ=0.3 the Exact Solution is $\|e\|_E^2$ = 1.46844

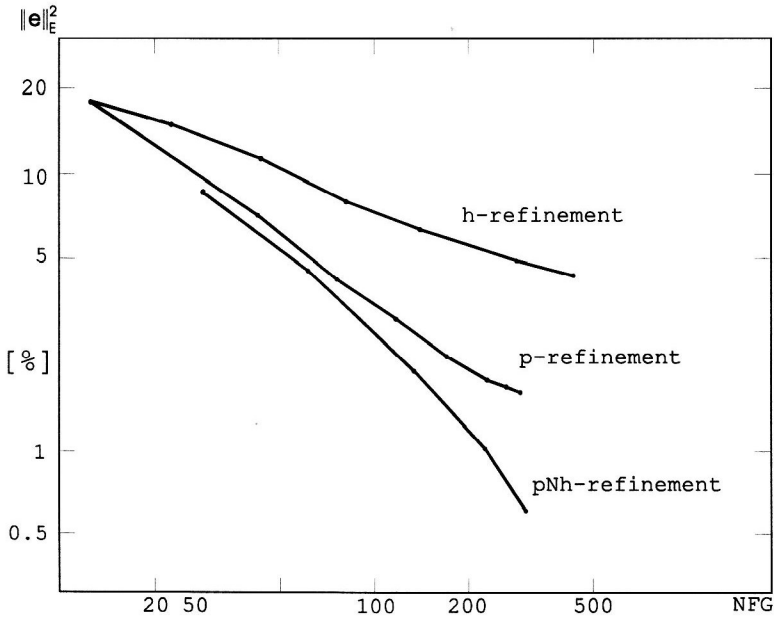

Figure 11. Convergency Rate of the Mesh Refinement

4.2 Contact of a Cylinder on a Elastic Foundation

The pNh-elements are especially suitable in solving contact problems within the p-version of the finite element method. Elasticity contact problems are non-linear due to the unknown contact area and consequently an iterative solution strategy is necessary to meet the static and kinematic contact conditions. A very fine linear h-refinement over the possible contact area is required to achieve a sufficient accuracy. In the contact area we use artificial finite bond elements with linear shape functions and normal and tangential contact stiffness (see Buczkowski et al, 1994; Gabbert et. al., 1993, 1994). As an example we present the solution of a classical Hertzian problem – the contact of an elastic cylinder with an elastic infinite foundation. To demonstrate the advantages of the pNh-elements we use a usual h-refined mesh in the halfspace and a coarse p-element mesh in the

cylinder (Figure 12), where the two elements in the contact area are pNh-elements with 15 lincar parts in all. The results shown in Figure 12 fit very good with the well known Hertzian solution.

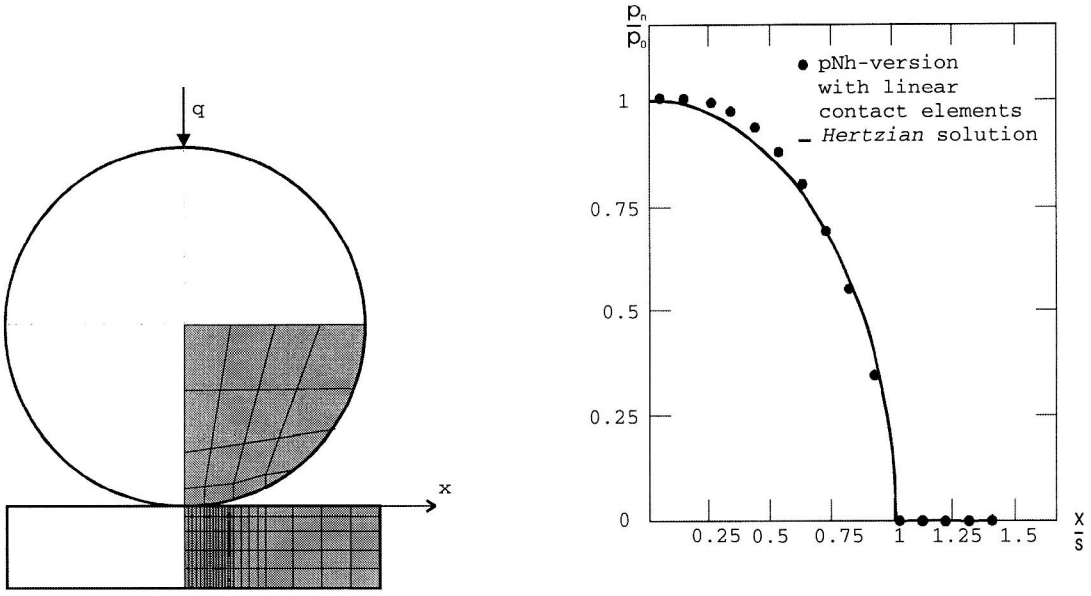

Figure 12. Cylinder on a Elastic Foundation

4.3 Pipe Branching

As a 3D example we demonstrate the calculation of a pipe branching. Close to the branch we have a complicated geometry and a complex three-dimensional stress state with high stress gradients. In a distance from the branch the stress distribution can be calculated with sufficient accuracy by means of the shell theory. A very accurate solution in the intersection region of the two pipes can be calculated with high efficiency by embedding a local h-refined mesh at the pipe branching as demonstrated in Figure 13. For details of the calculation see Graeff-Weinberg (1996). The example demonstrates that especially in 3D problems the pNh-elements are very suitable for carrying out adaptive local mesh refinements in a hp finite element techniques. By means of usual h-type finite element techniques such an effective mesh refinement is not possible.

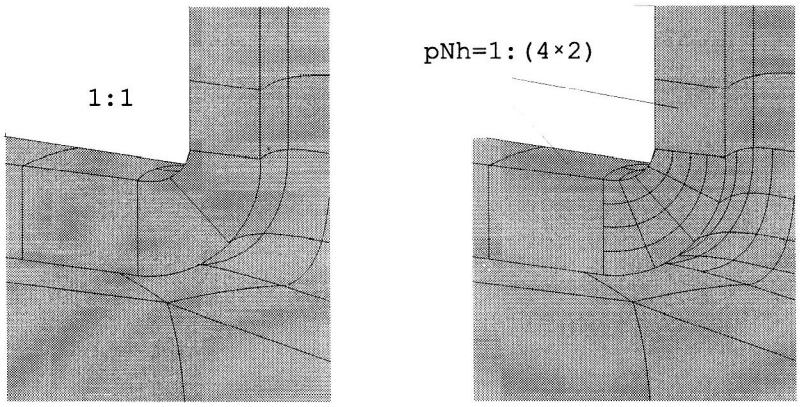

Figure 13. Mesh Refinement in a Pipe Branching with pNh-Elements

5 Conclusions

In the paper a new family of so called pNh-transition elements has been presented, which allows a compatible connection of differently meshed regions, especially coarse p-meshes with finite h-meshes. At one or more sides of a pNh-element a h-discretization with a number N of piecewise defined shape functions can be generated and at the other parts of the element any p-extension is possible. Consequently the pNh-transition elements can be regarded as a generalisation of p-version elements with a specially defined base function. The elements pass the patch test and can be used in an adaptive error controlled finite element scheme. The proposed pNh-elements

have been developed for 2D and 3D problems of elasticity, implemented and tested within a special finite element code as well as in a commercial code. A number of numerical tests and real engineering examples demonstrate the suitability, especially if strong local mesh refinements are required (e.g. multi-scale problems, contact problems etc.). The proposed finite element family can be seen as a contribution to the development of more intelligent finite element technologies in the future.

Acknowledgement: The work has been supported by the German Research Foundation (DFG). This support is gratefully acknowledged.

References

1. Babuška, I.; Rheinbold, C.: A-posteriori Error Estimates for the Finite Element Method, Int. J. Num. Meth. Engng., 12 (1978), pp. 1597-1615.

2. Babuška, I.: The p- and hp-version of the Finite Element Method – State of the Art, in R. G. Voigt, D. L. Dwoyer, M. Y. Hussaini (eds.), Finite Elements – Theory and Application, Springer, (1988).

3. Buszkowski, R.; Kleiber, M.; Gabbert, U.: On Linear and Higher Order Standard Finite Elements for 3D-Nonlinear Contact Problems, Computers & Structures, 53, No. 4, (1994), pp. 817-823.

4. Cavendish, J. C.; Hall, C. A.: A New Class of Transition Blended Finite Elements for the Analysis of Solid Structures, Int. J. Num. Meth. Engng., 20 (1984), pp. 241-253.

5. Fish: The s-version of the Finite Element Method, Computers & Structures, 43 (1992), pp. 539-547.

6. FEMCOS: Forschungsgesellschaft für Technische Mechanik mbH, Universelles FEM-System COSAR – Nutzerhandbuch, 2. Auflage, VECTOR Moritz & Pröbsting OHG, Hamburg, (1992).

7. Fels, D.; Gabbert, U.; Mücke, R.: Error Controlled Adaptive Mesh Refinement in 2D and 3D Finite Element Analysis, Proc. of the XXI. International Finite Element Congress FEM '92, November 16 and 17, Baden Baden, (1992).

8. Gabbert, U.; Graeff-Weinberg, K.: pNh-Elemente für die Lösung nichtlinearer Kontaktprobleme in der p-Version der FEM, Proc. of the XXII. International Finite Element Congress FEM '93, Baden Baden, Nov. 15 and 16, (1993).

9. Gabbert, U.; Graeff-Weinberg, K: Eine pNh-Elementformulierung für die Kontaktanalyse, ZAMM 74, issue 4, (1994), T195-T197.

10. Gabbert, U.; Zehn, M.: Adaptive Remeshing Based on Error Estimations – Foundations, Implementation and Application, Proc. of NAFEMS 5th International Conference on Reliability of Finite Element Methods for Engineering Applications. Amsterdam, 10-12 May, (1995), pp. 1-10.

11. Gabbert, U.; Wahl, F.; Zehn, M.: Improved Results in Structural Dynamic Calculations by Linking Finite Element Analysis (FEA) and Experimental Modal Analysis (EMA), Proc. of the ASME Design Engineering/Technical Conferences, DE-Vol. 84-3, Boston, (1995), pp. 1321-1328.

12. Gordon, W. J.: Blending Function Method of Bivariate Interpolation and Approximation, SIAM J. Num. Meth. Anal. 8, (1971), 158-177.

13. Graeff-Weinberg, K.: Ein Finite-Element-Konzept zur lokalen Netzverdichtung und seine Anwendung auf Koppel- und Kontaktprobleme, Dissertation, Universität Magdeburg, (1996).

14. Mücke, R.: Beitrag zur Berechnung linearer Elastizitätsprobleme mit h-adaptiven Finite-Element-Verfahren, Dissertation, Universität Magdeburg, (1992).

15. Jensen, S.: Computational Aspect of Adaptive Dimensional Reduction for Nonlinear boundary value Problems, in J. Robinson (Ed.): Finite Element Methods in the Desgn. Process, Robinson & Associates, Okehampton, (1990).

16. Mottershead, J. E.; Friswell, M.: Model updating in Structural Dynamics: A survey, J. of Sound and Vibration 167 (2), (1993), 347-375.

17. Oden, J. T.; Demkowicz, L.; Rachowicz, W.; Hardy, O.: Toward a Universal h-p Adaptive Finite Element Strategy, Part 1: Constraint Approximation and Data Structure, Part 2: A Posteriori Error Estimation, Part 3: Design of hp-Meshes, Computer Meth. in Appl. Mech. and Engn. 77 (1989), 79-112, 113-180, 181-212.

18. Stein, E.; Ohnimus, S.: Dimensionsadaptivität bei Finite-Element-Berechnungen von Stäben und Platten, ZAMM, 73, (1993), T673-Z677.

19. Stein, E.; Ohnimus, S.: Expansion Method for the Integrated Solution and Model Adaptivity within the FE-Analysis of Plates and Shells, in N.-E. Wiberg (Ed.): Advances in Finite Element Technology, CIMNE Barcelona, (1995).

20. Szabo, B. A.; Babuška, I.: Finite-Element-Analysis, John Wiley & Sons, (1991).

21. Wiberg, N.-E.: Superconvergent Patch Recovery of Finite Element Solution and a Posteriori Error Estimate, Commun. Num. Meth. Engng., 10, (1994), pp. 313-320.

22. Zienkiewicz, O. C.; Zhu, J. Z.: A Simple Error Estimator and Adaptive Procedure for Practical Engineering Analysis. Int. J. Num. Meth. Engng., 24, (1987), pp. 337-357.

23. Zienkiewicz, O. C.; Zhu, J. Z.: The Superconvergent Patch Recovery and a Posteriori Error Estimators. Part I: The Recovery Technique, Part II: Error Estimates and Adaptivity, Int. J. Num. Meth. Engng., 33, (1992), pp. 1331-1382.

24. Zienkiewicz, O. C.: The Finite Element Method, McGraw-Hill Book Company (UK), (1977).

Address: Prof. Dr.-Ing. Ulrich Gabbert and Dr.-Ing. Kerstin Graeff-Weinberg, Institut für Mechanik, Otto-von-Guericke-Universität Magdeburg, Universitätsplatz 2, D-39106 Magdeburg